Asian Journal of Geological Research

2(3): 225-238, 2019; Article no.AJOGER.53873

Hydrocarbon Reservoir Characterization and Modelling, Akos Field, Niger Delta, Nigeria

Enyenihi Emmanuel Enifome[1], Emujakporue Godwin Omokenu[1*] and L. I. Nwosu[1]

[1]Department of Physics, University of Port Harcourt, Rivers State, Nigeria.

Authors' contributions

This work was carried out in collaboration among all authors. Author EEE designed the study, performed the statistical analysis, wrote the protocol and wrote the first draft of the manuscript as part of his MSc research. Author EGO supervised the work and assisted in preparing the manuscript. Author LIN helps in interpreting the results and editing the manuscript. All authors read and approved the final manuscript.

Article Information

Editor(s):
(1) Dr. Ahmed Abdelraheem Frghaly, Associate Professor, Sohag University, Egypt.
(2) Dr. Adewumi, Adeniyi John Paul, Lecturer II, Department of Geological Sciences, Achievers University, Owo, Nigeria.
Reviewers:
(1) Rogério Porciúncula, Universidade Federal do Recôncavo da Bahia (UFRB), Brazil.
(2) Safaa Fakhir Yasir Al-Ghnaimawi, Universiti Teknologi MARA, Malaysia.
(3) Fábio Henrique Portella Corrêa de Oliveira, Universidade Federal Rural de Pernambuco, Brazil.
Complete Peer review History: http://www.sdiarticle4.com/review-history/53873

Original Research Article

Received 18 November 2019
Accepted 22 January 2020
Published 27 January 2020

ABSTRACT

In this research, seismic and well logs data were used for constructing a 3-D static reservoir model of Akos-Field, The aim was to generate the structural and petrophysical models of the delineated reservoirs. The reservoir modeling involves the integration of structural information and rock properties using geostatistical techniques. Two reservoirs A and B were observed in the well logs. Fault polygons were used in building the structural model. The lithological facies architecture was simulated using a sequential indicator while the porosity, net to gross, water saturation and permeability modeling were simulated with sequential Gaussian simulation. The modeling shows that reservoir B has good petrophysical data distribution than reservoir A. The STOIIP estimation shows that the approximate volume of hydrocarbon that can be obtained in reservoirs A and B are $23.33\times10^{6}m^{3}$ and $72.22\times10^{6}m^{3}$ Stock Tank Barrels (STB) respectively. The results show that the Akos field has hydrocarbon potential for development.

**Corresponding author: Email: owin2009@yahoo.com;*

Keywords: 3D Petrophysical model; geostatistical method; seismic data; well logs.

1. INTRODUCTION

Reservoir description and characterization involved mapping of the petrophysical properties. The process requires the construction of a detailed 3D petrophysical property models contained within a geological framework. The structural interpretation of seismic data is very essential in producing a hydrocarbon reservoir framework. Seismic, well log, and core data are usually combined in reservoir characterization to unravel the structure of the reservoir and the nature of the fluid in it [1,2,3]. A geoscientist uses several available data to create a model for describing the structure of the rocks in the subsurface [4]. Static reservoir modeling involves structural, stratigraphic, facies and property modeling [5]. Spatial distribution of petrophysical properties in the reservoir is difficult to predict deterministically [6,7,8,9]. Hydrocarbon reservoirs properties distribution can be determined by deterministic and probabilistic modeling [10,11,12,13].

The objective of this study is to used available well log and seismic data to build a reservoir static model of the Akos field. Accurate and reliable characterization and modeling are very important in hydrocarbon production optimization. Currently, the integration of different kinds of dataset to obtain an accurate and robust reservoir model is a major challenge.

Geostatistical modeling was used to characterize the reservoir. The geostatistical techniques are normally used in reservoir modeling to unravel the diversity and heretogeneity of a complex reservoir. It is useful in identifying data limitation and provides a good description of reservoir complexity. Geostatistical tools are particularly effective when dealing with data sets with vastly different degrees of spatial density and diverse vertical and horizontal resolution. A variogram is a major tool of geostatistics and it is an estimation of dissimilarity between sampled data [14,15,16].

2. SUMMARY OF THE GEOLOGY OF NIGER DELTA

The Akos field is situated in onshore coastal swamp depositional belt, eastern parts of Niger Delta (Fig. 1) and it is located within latitudes 4°19′ N and 4°50′ N and Longitudes 6°02′30" E and 7°10′00" E. The base map is shown in Fig. 2.

The Niger-Delta which covers an area between longitude 4 – 9º E and Latitude 4 - 9º N, is a major Hydrocarbon provinces and it is situated on the Gulf of Guinea on the west coast of Africa. It has an area of 75,000 km^2 with an average thickness of about 12 km. It is composed of an overall regressive clastic sequence.

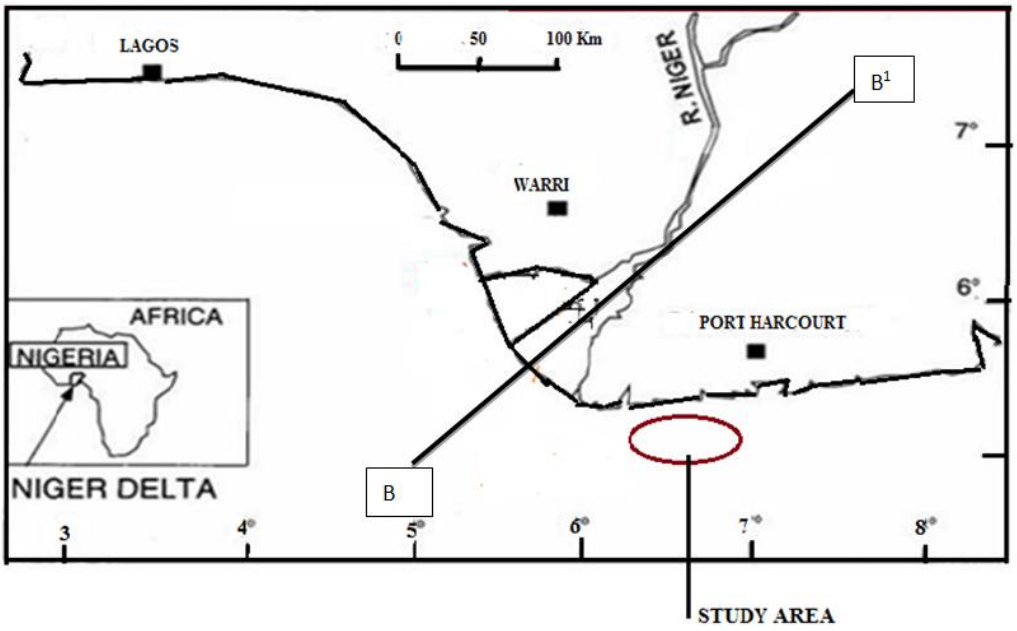

Fig. 1. Map Niger Delta showing the study area

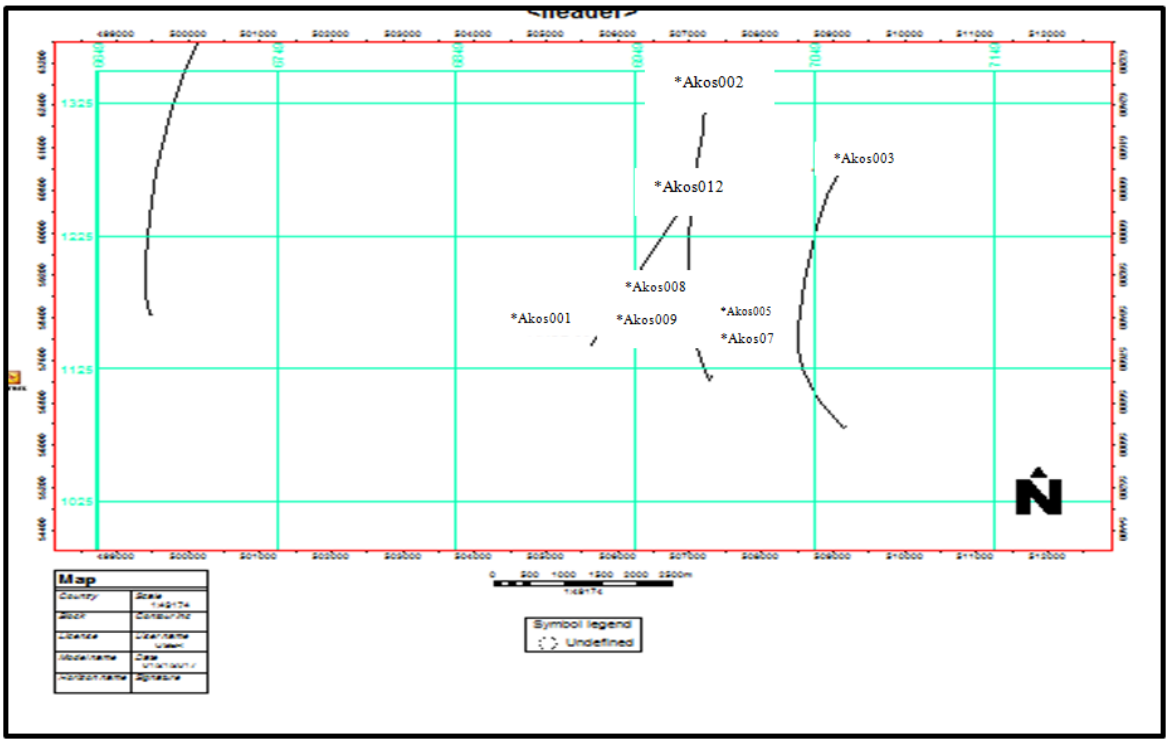

Fig. 2. Base map showing the seismic lines and well locations

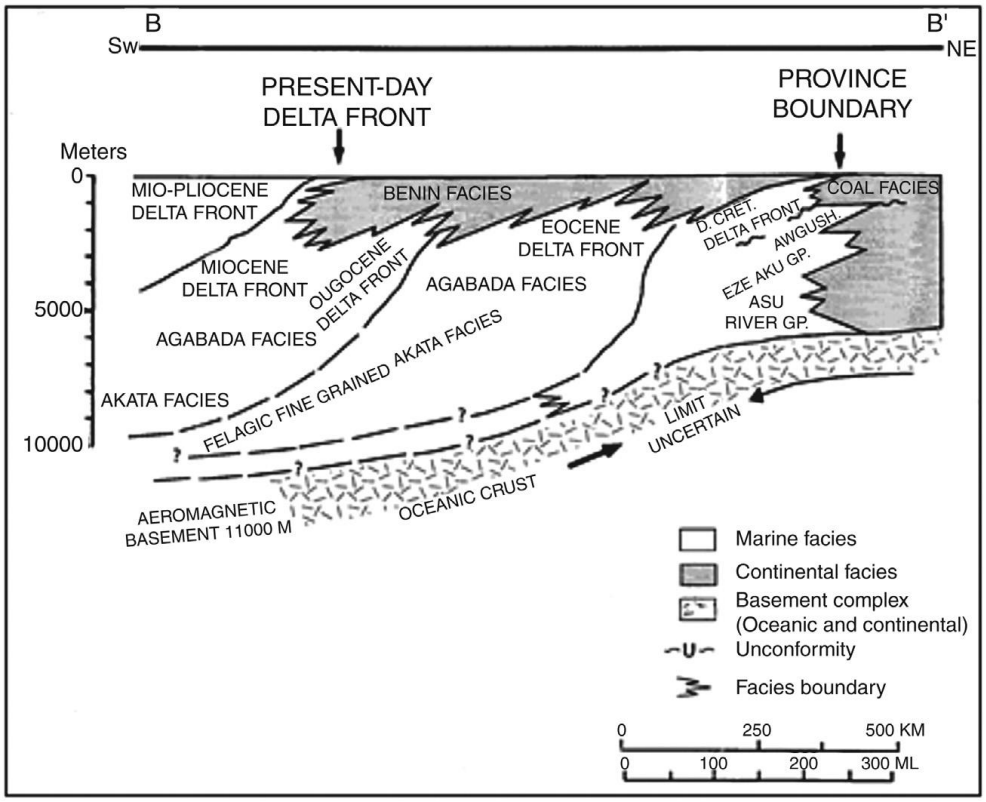

Fig. 3. Dip section of the Niger Delta showing the structural provinces of the Delta
[Adapted from 22]

The Tertiary Niger Delta (Akata-Agbada) petroleum system is the only identified petroleum system [17,18,19,20,21]. Growth faults are the most common geological features of the Niger Delta. The Niger Delta hydrocarbon province is characterized by East-West trending synsedimentary faults and folds. Most of the oil accumulated in the Niger Delta is contained in the rollover anticline structures. The oil in these structures may be trapped in dip closures or against a Synthetic or antithetic fault (Fig. 3).

3. MATERIALS AND METHODS

The dataset used for this research consists of composite logs from eight exploratory oil wells and 3D seismic volume. The composite log is made up of gamma-ray, resistivity and bulk density logs. The following workflow techniques was adopted for the research; structural, property and petrophysical modeling using geostatistical techniques in Petrel software.

3.1 Determination of Lithology and Reservoir

The formation lithology and reservoir were delineated with the aid of the available gamma-ray and resistivity logs. Deflection of the gamma ray log to left (low values) indicates sandstone while the deflection to the right (high values) represents shale. High resistivity values coinciding with a sandstone zone is an indication of reservoir sand while low resistivity values represent shale or reservoir containing saltwater. The gamma ray log was used for estimating the reservoir thickness.

3.2 Determination of Porosity

Porosity is a major parameter used for estimating the amount of hydrocarbon in a reservoir. The density log was used for estimating the porosity of the reservoir by applying the equation [23,24]

$$\Phi = \frac{(\rho_{max} - \rho_b)}{(\rho_{max} - \rho_{fl})} \quad (1)$$

Where

Φ = porosity derived from density log
ρ_{max} = matrix density (2.65 g/cm^3)
ρb = bulk density (as measured by the tool and hence includes porosity and grain density)
ρfl = fluid density (1 g/cm)

3.3 Determination of Fluid Saturation

The fluid saturation of a reservoir depends on the pore space. The pore space may be occupied by water, oil and /or gas. The amount of hydrocarbon saturation, in the reservoir depends on the water saturation. Water saturation is the fraction of pore space occupied by formation water. Water saturation can be obtained from porosity by using the equation [25],

$$S_w = \frac{0.082}{\Phi} \quad (2)$$

Where,

S_w = water saturation
Φ = effective porosity

The hydrocarbon saturation in the reservoir is obtained as the difference between unity and fraction of water saturation [26,24] and it is given as;

$$S_h = 1 - S_W \quad (3)$$

The water saturation can be express as a fraction or percentage. In percentage form, it is given as;

$$S_h\ \% = 100 - S_w\% \quad (4)$$

Where

S_h= hydrocarbon saturation
S_w = water saturation

3.4 Determination of Permeability

Permeability is simply a measure of the ease with which a formation allows fluid to flow through it via its interconnected pores, vugs, capillaries, fissures or fractures (Pore throat). The permeability values for the observed reservoirs were calculated using the equation after [27]:

$$K = 307 + (26552 * \phi^2) - (34540 * [\phi * S_{wirr}]^2) \quad (5)$$

Where

K = Permeability
ϕ = porosity
S_{wirr} = Irreducible water saturation

3.5 Reservoir Modeling

Static reservoir modeling was applied to the calculated petrophysical data to distribute the petrophysical properties in the 3D grid. There are two types of interpolation techniques: Deterministic and geostatistic. The two techniques depending on the similarity of the nearby sample points are used to create the heterogeneity of the reservoir properties. Geostatistics routines are implemented in the major reservoir modeling packages like Petrel used in the generation of grids for facies, permeability and porosity, of the reservoir. In this study variogram and simple kriging techniques were adopted to generate petrophysical properties distribution maps. Petrophysical property modeling involves the distribution of porosity, water saturation, NTG, and permeability values to every cell of the 3D grid. It is a technique of filling the cells of the grid with distinct (Rock type) or continuous (Petrophysics) properties. The 3D property modeling depends on information obtained from well logs. The Petrophysics models generated for this work include:

3.5.1 Porosity modeling

Porosity model was constructed based on the values of porosity logs computed from the density logs. Sequential Gaussian Simulation was used for distributing the porosity values within the cells created from the seismic interpretation.

3.5.2 Water saturation modeling

Water saturation model was built from the values obtained from the formation evaluation. Statistical Gaussian Simulation Algorithm was used for the distribution of the water saturation in the 3D grid.

3.5.3 Facies modeling

Facies modeling involves distributing discrete facies throughout the model grid. The lithology observed in the reservoir were distributed with the geostiscal techniques.

3.5.4 Permeability model

Permeability is very essential in reservoir rock characterisation. It determines the ability of a formation to transmit fluids. The computed permeability values were distributed in the cells using geostatistical algorithm in the software.

3.5.5 Net to gross ratio

The net to gross ratio model for delineated reservoirs were also calculated and distributed in the 3D grid.

3.6 Variogram Method

Variogram is used for computing and describing the spatial variations of reservoir properties. It helps to infer the continuity of petrophysical properties in a reservoir. The experimental variogram is given as

$$\gamma(h) = \frac{\sum_{i-1}^{N(h)} \left(x_i - x_{i+h}\right)^2}{2N(h)} \quad (6)$$

where

$2\gamma(h)$ = variogram,
$xi + h$, xi: = variables x at location i and $i + h$,
h = lag vector,
$N(h)$ = number of pairs.

The experimental variogram is not enough for spatial analysis and therefore suitable theoretical models were fitted on it. Different models such as exponential, gaussian and spherical were fitted on the experimental variogram and the best one was used for the kriging analysis;

3.7 Kriging Method

Kriging is a geostatistical estimation techniques and it is known as the best-unbiased estimator. It has the least estimation variance. Kriging is based on weighted moving average and it can be obtained the equation [28]

$$Z_v^i = \sum_{i-1}^{n} \lambda_i Z_{iv} \quad (7)$$

Where

Z_v^i = grade estimation,

λ_i = weight or importance of the value

Z_{iV} = the grade of the ith sampled.

Equation (5) was the model used for the distribution of petrophysical data.

3.8 Construction of 3D Grids for the Horizons

The seismic data was interpreted for horizons and faults. The observed faults were modeled and pillar to generate 3D grids for the identified horizons. Fault modeling involves digitizing and displaying all fault skeletons according to their trends in the field. The faults were interpreted using fault sticks while fault trends were built using pillars.

3.9 Estimation of Reservoir Volume

Estimating the quantity of hydrocarbon in the reservoir is a very important stage in the modeling process as it helped in making decision on the best reservoir bearing hydrocarbon. This is very important because it acts as a guide for field exploration and development. After a static model of a field was done, the structural model and the petrophysical model built were used to calculate reserves in terms of Stock Tank of Oil Initially In Place (STOIIP) [22].

$$STOIIP = \frac{7758 \times Area \times Thickness \times Porosity(1 - S_w) \times NTG}{FVF} \quad (8)$$

Where:

STOIIP (mmstb) = stock tank oil initially in place
Sw= water saturation
NTG = net-to-gross ratio
FVF = formation volume factor (a constant)

4. RESULTS AND DISCUSSION

Two reservoirs (A and B) were delineated and correlated across the well logs (Fig. 4). The lithologies observed in the gamma ray logs are mainly sand and shale. Figs. 5 and 6 show some of the interpreted seismic data used for the reservoir modeling.

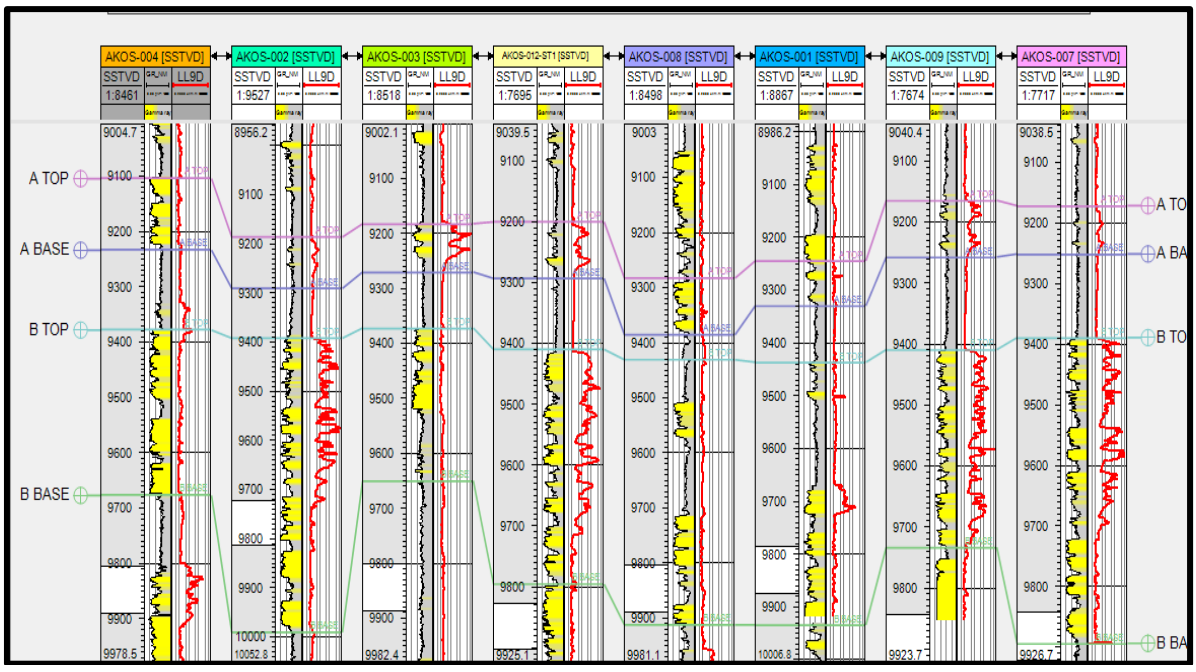

Fig. 4. Well log correlation panel of Akos field

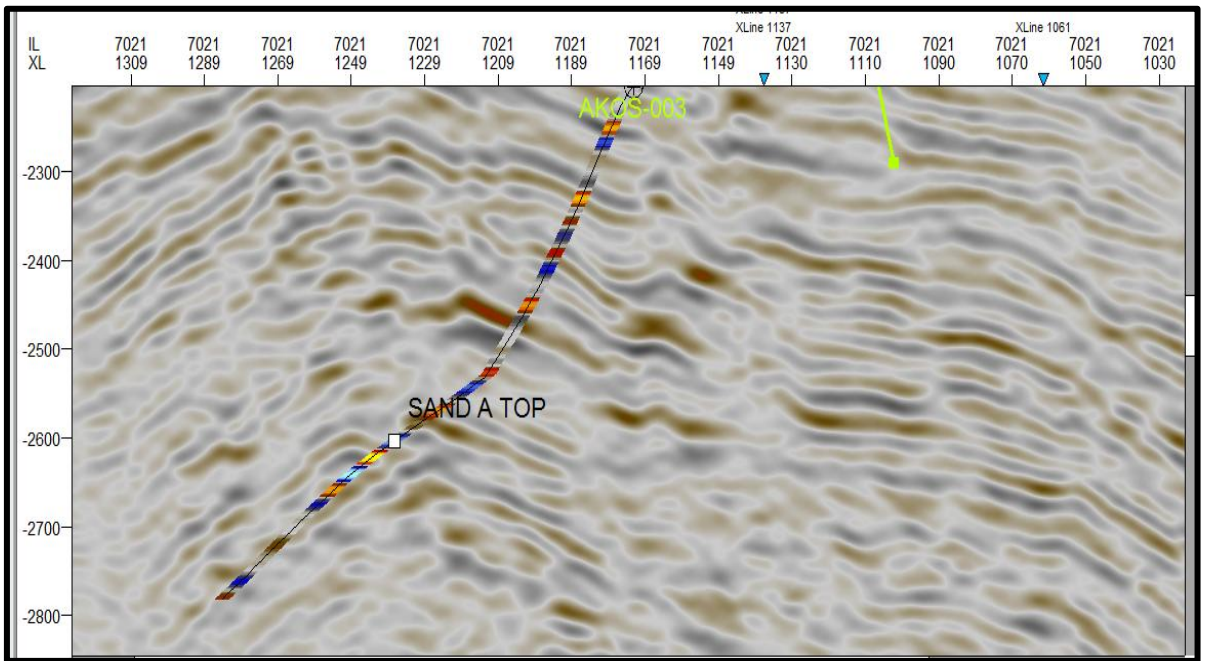

Fig. 5. Well-to-seismic tie on Inline 7021

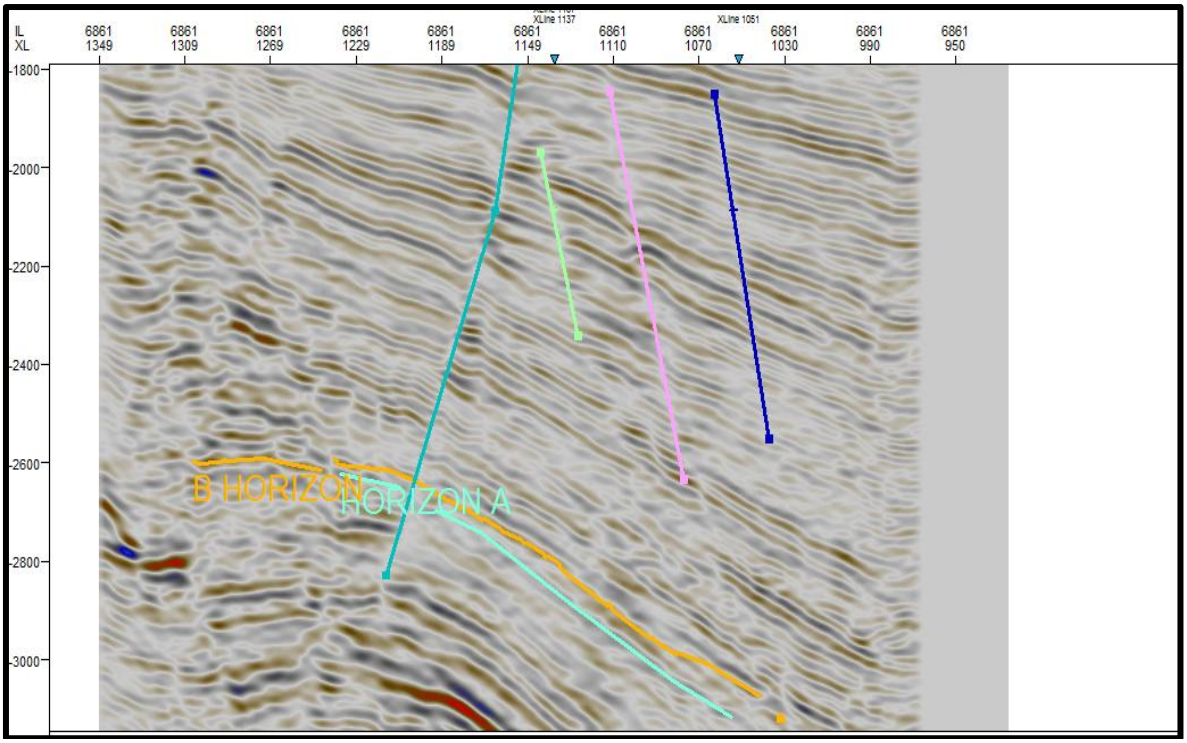

Fig. 6. Interpreted seismic section showing the horizons and faults in Inline 6861

4.1 Structural Reservoir Modeling

Faults are identified on the dip seismic sections, in the interpretation 3D window. Eight faults were delineated in the seismic volume out of which six are major and two minor. The interpreted faults were modeled and pillar gridded. These faults were used to generate 3D grids for the horizons. The grids generated for reservoirs A and B are shown in Figs. 7 and 8 respectively. Each of the grid cells has a single rock type one value of porosity, one value of permeability, one value of

water saturation and one value of NTG. It means the generation of the structural model was done the process of pillar gridding preserves small features from well logs and seismic data. Pillar gridding makes it possible to delineate the top, middle, and base of the structural model.

4.2 Property Modeling

The property modeling involves the generation of facies, porosity, water saturation, permeability and net to gross models.

4.3 Facies Model

The generated facies model for reservoirs A and B are shown in Figs. 9 and 10. The facies observed in the reservoirs are shale (coloured grey), fine sand (coloured brown) and sand (coloured yellow). The map shows that for reservoir A, the northeast flank is dominance with shale while the northwest is dominated with sand. Reservoir B is dominated with sand. Reservoir B denotes a good prospect of hydrocarbon due to the high occurrence of sand which implies high porosity and permeability than reservoir A. The shale facie in reservoir A will act as to seal to the flow of fluid.

4.4 Porosity Model

The 3D porosity model for reservoirs A and B are shown in Figs. 11 and 12. The models show good porosity distribution (blue coloration) in the central region, north-west and south-east flanks for reservoir A while reservoir B have almost a uniform high distribution of porosity.

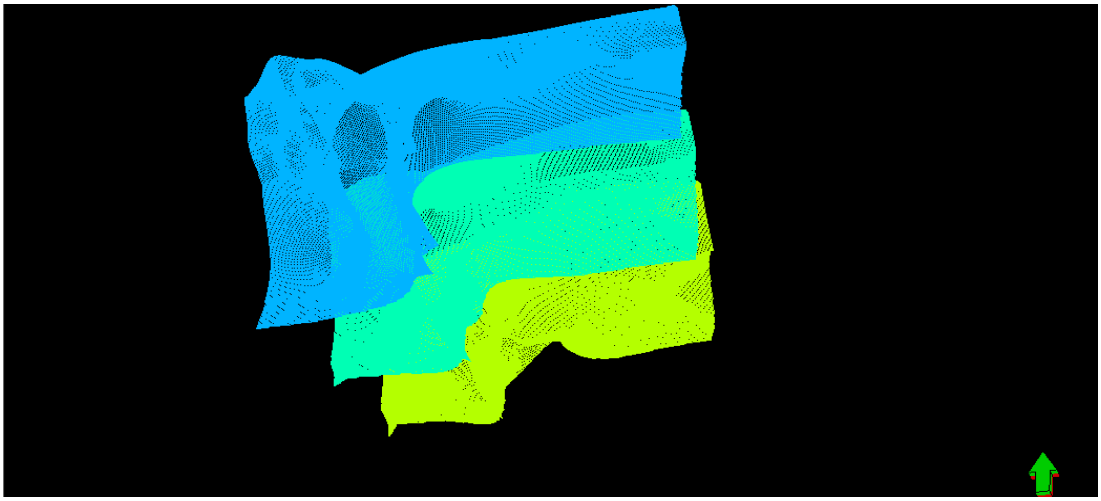

Fig. 7. Reservoir A pillar gridding

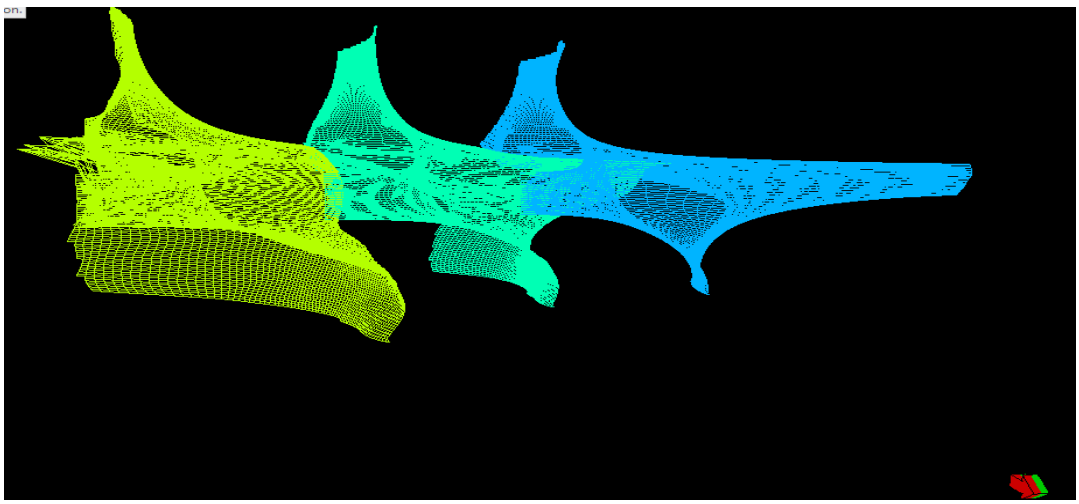

Fig. 8. Reservoir B pillar gridding

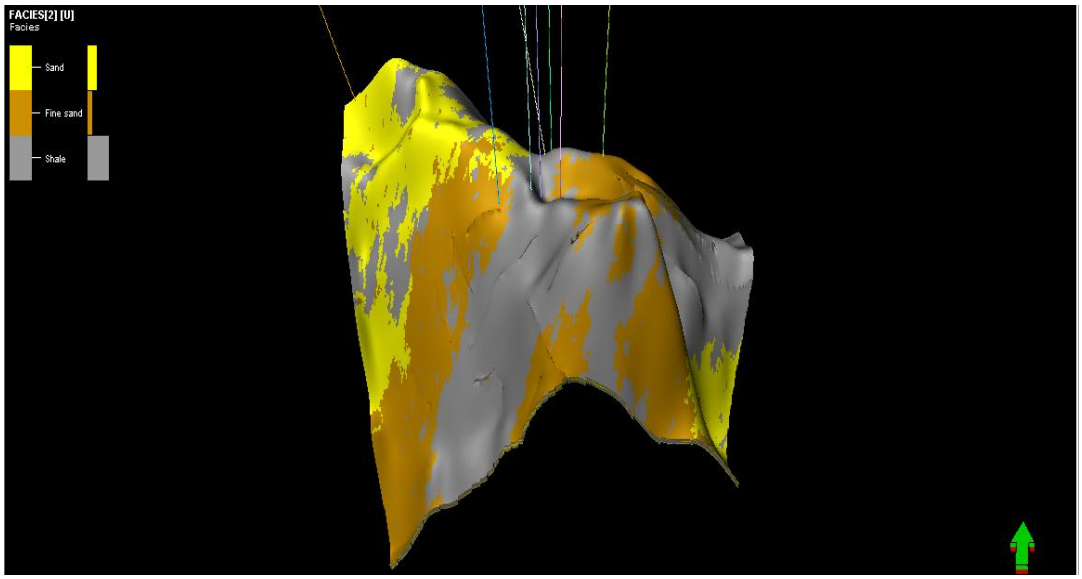

Fig. 9. Facies model for reservoir A

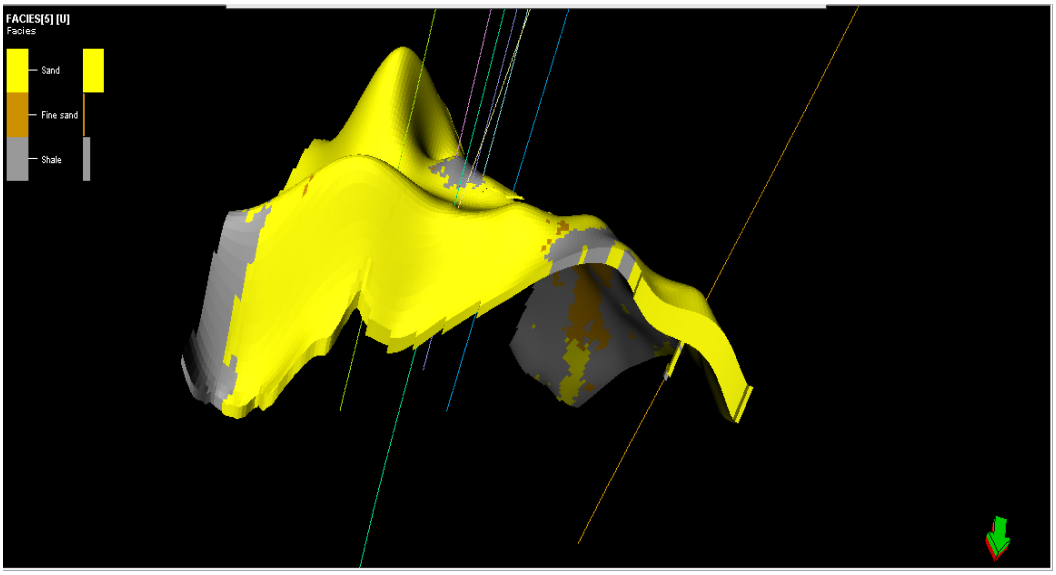

Fig. 10. Facies model for reservoir B

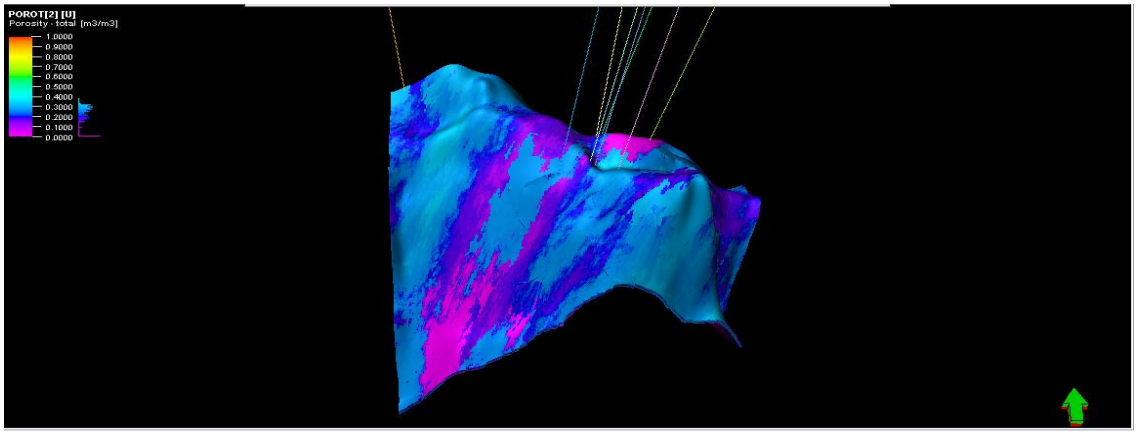

Fig. 11. Porosity model for reservoir A

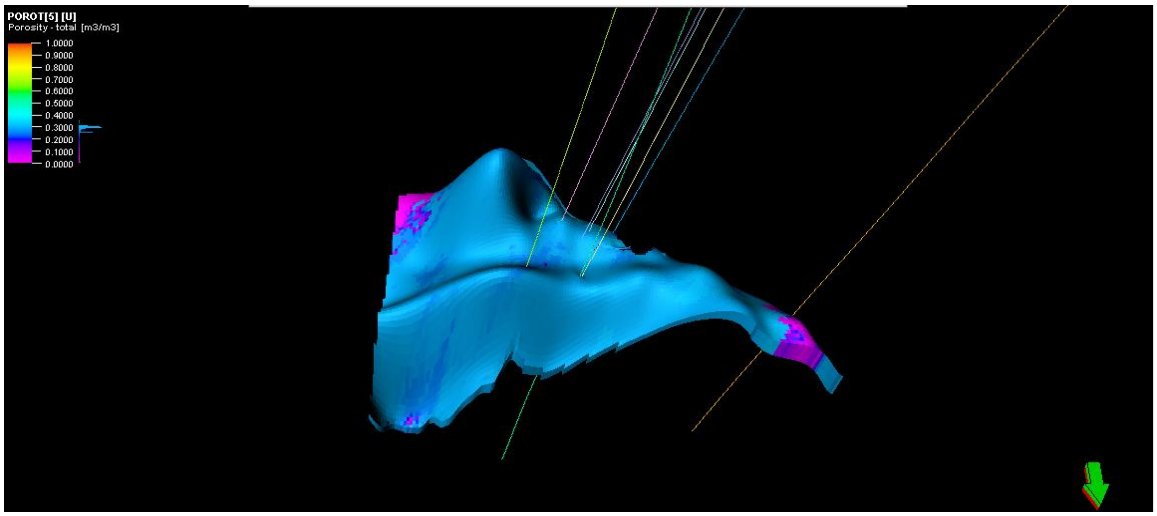

Fig. 12. Porosity model for reservoir B

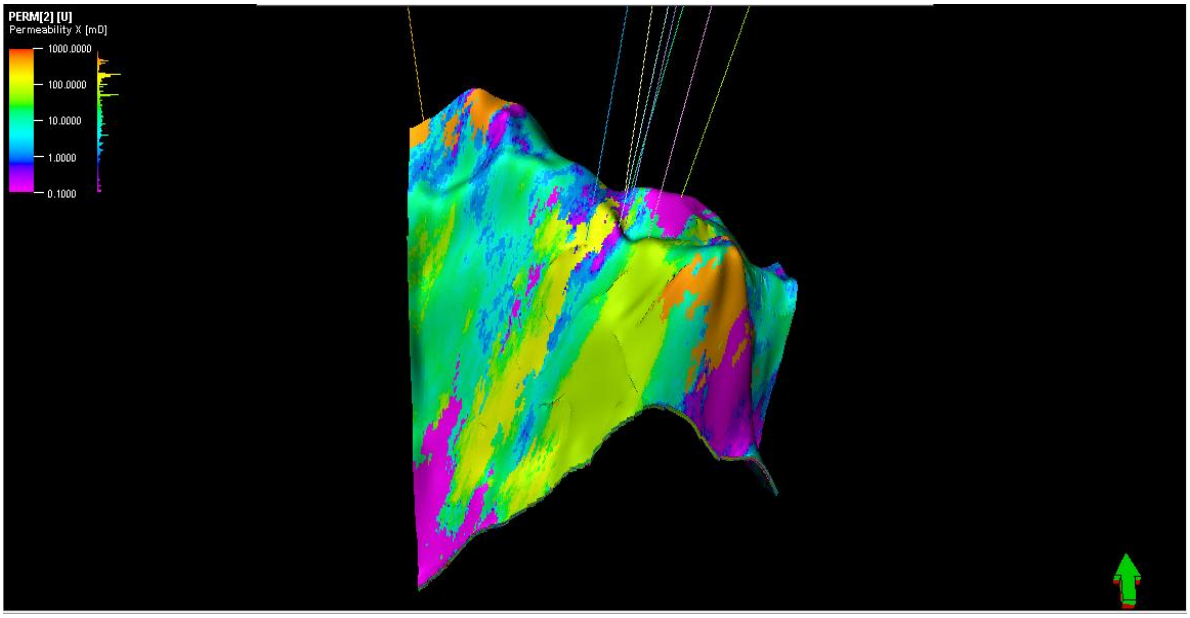

Fig. 13. Permeability model for reservoir A

4.5 Permeability Model

Figs. 13 and 14 show the permeability models for reservoirs A and B. The high permeability regions are denoted with yellow/green and red colorations. Reservoir A has a yellow/green distribution in the central region and also trending in the southeast flank. Reservoir B has high permeability (yellow/green) in the north-west and southeast regions. The models show that reservoir B has good permeability which is good for hydrocarbon prospecting. Reservoir A will have some challenge during drilling because of the low permeability zones.

4.6 Water Saturation Model

Figs. 15 and 16, show the 3D view of the water saturation of reservoirs A and B. The maps reveal that high water saturation is indicated with green and blue colorations which signify low hydrocarbon saturation. The yellow coloration depicts low water saturation which is an indication of high hydrocarbon saturation. Reservoir A shows a high percentage of green coloration evenly distributed and a small portion of yellow coloration in the south-west region. Reservoir B has very high green coloration distributed in the central and north-west regions.

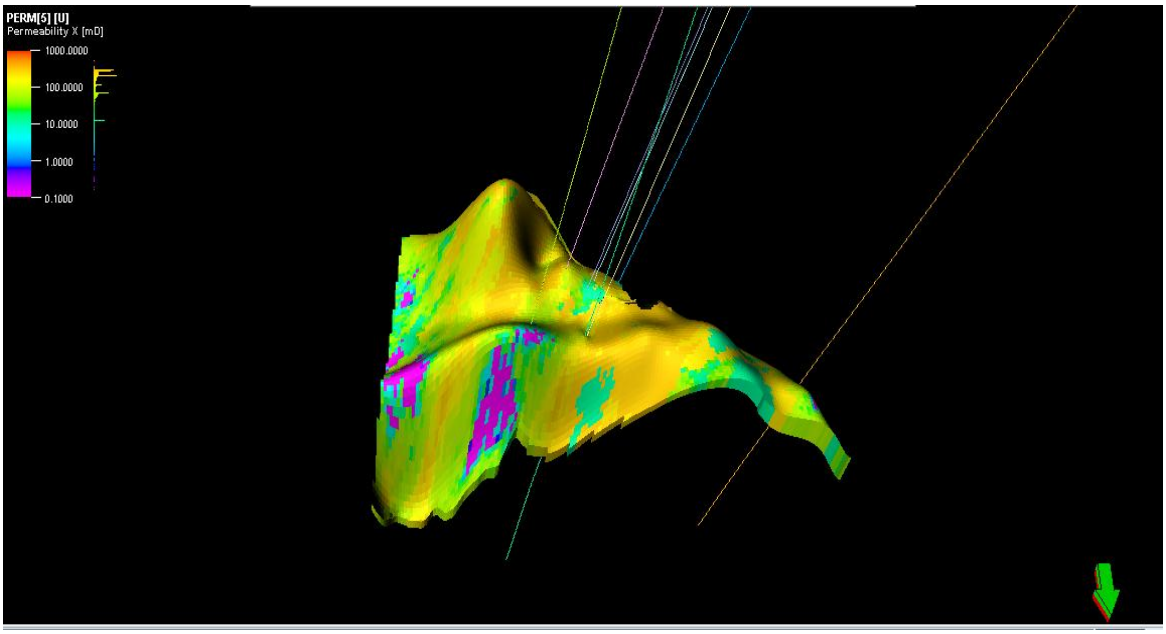

Fig. 14. Permeability model for reservoir B

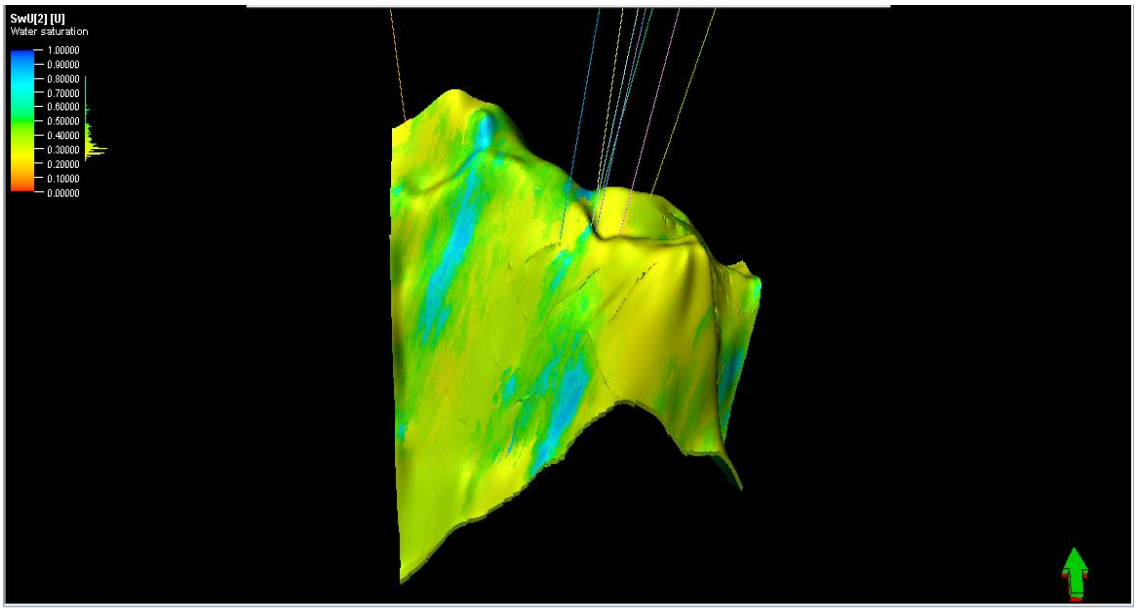

Fig. 15. Water saturation model for reservoir A

Table 1. Computed average petrophysics parameters of reservoirs A and B

Reservoir	Thickness (ft)	Porosity (fraction)	Permeability (mD)	Sw (fraction)	NTG (fraction)	STOIIP (mmstb)
A	116	0.286821	253.1797	0.305543	0.433562	23.33
B	489	0.245688	162.7688	0.36655	0.44595	72.22

4.7 Net to Gross Model

Net to gross (NTG) is the measure of the reservoir volume occupied by hydrocarbon bearing rocks. It shows the volume of shale present in the reservoir. Figs. 17 and 18 are the Net to gross for reservoirs A and B respectively. The reservoirs denote a good prospect evident

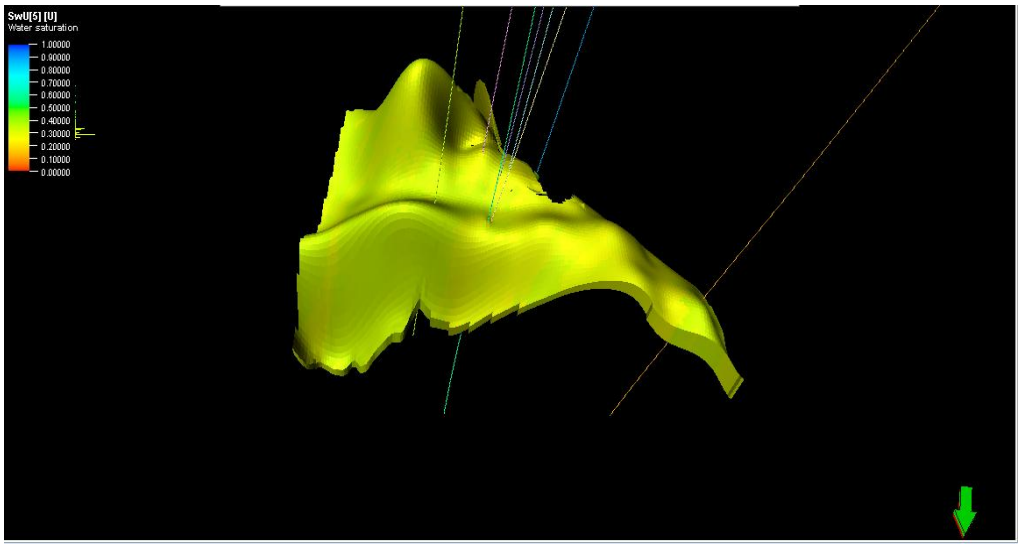

Fig. 16. Water saturation model for reservoir B

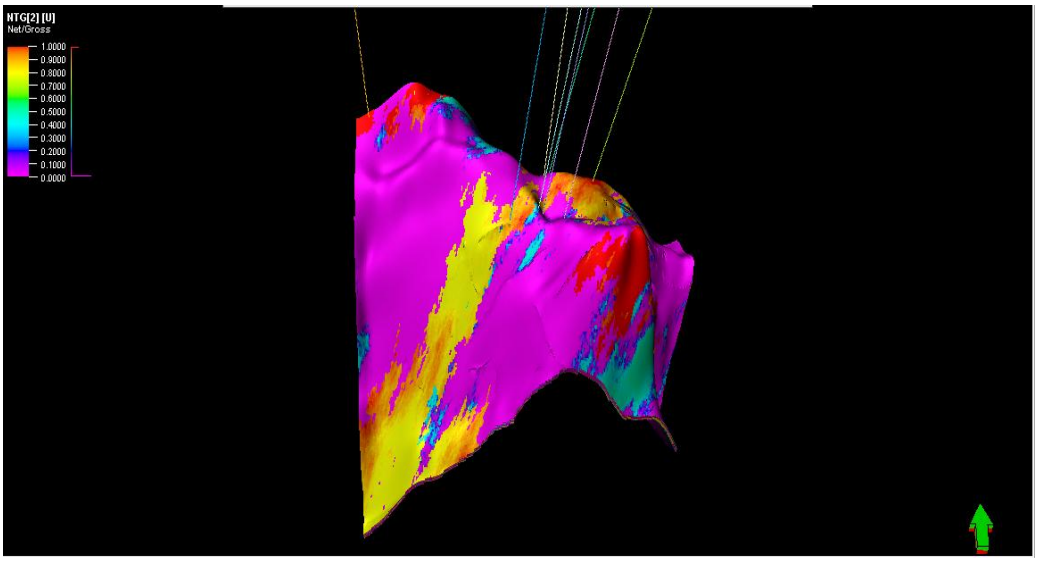

Fig. 17. Net-to-gross model for reservoir A

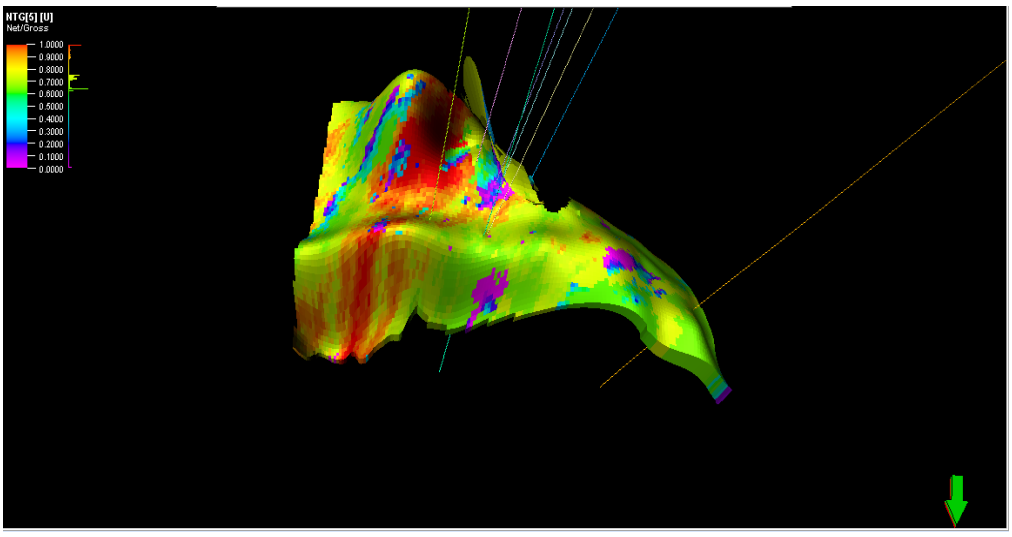

Fig. 18. Net-to-gross model for reservoir B

from their high net-to-gross value. Reservoir A shows red/yellow coloration in the central and southeastern flank while reservoir B shows yellow/red coloration at the central and northwestern flank. The high Net to gross values is an indication for high hydrocarbon saturation value.

4.8 Volume Estimation

The computed average petrophysics parameters for reservoirs A and B are shown in Table 1. The result shows that the average petophysical properties of the reservoirs are good. The volume of hydrocarbon obtained in Reservoir A is $23.33\times10^6 m^3$ and Reservoir B is $72.22\times10^6 m^3$ Stock Tank Barrels (STB). The reservoir static model could be used as input data for simulation and performance.

5. CONCLUSION

The integration of available geophysical, geological, and petrophysical data has led to the building of a consistently high resolution 3-D static model of the delineated reservoirs in the study area. The 3-D model can be better applied in well planning compared with the 2-D reservoir map conventionally used for the same purpose. The results of the study show that the field has good structural and petrophysical parameters for hydrocarbon potential. The geomodeling has led to a detailed description and characterization of the reservoirs and the results can be used by reservoir engineers for further effective and economic management of the reservoirs.

COMPETING INTERESTS

Authors have declared that no competing interests exist.

REFERENCES

1. Ezekwe JN, Filler SL. Modelling deepwater reservoirs, paper SPE 95066 presented at the 2005 SPE Annual Technical Conference and Exhibition held in Dallas, Texas, U.S.A. 2005;9–12.
2. Mehdipour V, Ziaee B, Motiei H. Determination and distribution of petrophysical parameters (PHIE, Sw, and NTG) of the Ilam Reservoir in one Iranian oil field. Life Sci. J. 2013;10:153-161.
3. Hadi J, Harrison C, Keller J, Rejeki S. Overview of darajat reservoir characterization: A volcanic hosted reservoir. Proceedings of the World Geothermal Congress Antalya, Turkey. 2005;1-11.
4. Gadallah M, Fisher R. Exploration Geophysics, Springer-Verlag. 2009; Berlin Heidelberg.
5. Maucec M, Yarus J.M, and Chambers Next generation modeling for hydrocarbon reservoir characterization, Halliburton energy services Graporation, USA; 2013.
6. Miller RB, Castle JW, Temples TJ. Deterministic and stochastic modeling of aquifer stratigraphy, South Carolina. Groundwater. 2000;38.
7. Ma SM, Zeybek MM, Kuchuk FJ. Integration of static and dynamic data for enhancing reservoir characterization, geological modeling and well performance studies. Saudi Aramco Journal of Techn. 2013;62-69.
8. Adeoti L, Onyekachi N, Olatinsu O, Fatoba J, Bello M. Static reservoir modeling using well log and 3-D seismic data in a KN field, offshore Niger Delta, Nigeria. Int. J. Geosci. 2014;5:93-106.
DOI: 10.4236/ijg.2014.51011
9. Qihong L, Ziqi S, Chengqian T. Reservoir description of the stochastic simulation method [J] Journal of Xi'an Petroleum Institute (Natural Science Edition). 2000;15(1):13-16.
10. Godwill PA, Waburuko J. Application of 3D reservoir modeling on Zao 21 Oil Block of Zilaitun oil Field. J. of Pet Environ Biotechnol. 2016;7:262.
DOI: 104172/2157-74631000262. 8p
11. Perevertailo T, Nedolivko. N. Prisyazhuyuk O, Dolgaya T. Application of geologic mathematical 3D modeling for complex structure deposits by the example of lower Cretaceous period depositions in western Ust-Balykh oil field (Khanty- Mansiysk Autonomous District). IOP conference series: Earth and Environmental Science. 2015;27.
DOI:10.1088/1755.1315/27/1/012016. 5p
12. Kelka M, Perez G. Applied Geostatistics for Reservoir Characterization. 1st Edn., Society of Petroleum Engineers, Richardson; 2002.
[ISBN - 10:2002;264]
13. Başel E, Korkmaz D, Satman A, Serpen U. Predicted subsurface temperature distribution maps for Turkey. Proceedings

world geothermal congress, Bali, Indonesia. 2010;1-7.
14. Deutsch CV. Geostatistical reservoir modeling, Oxford University Press. 2002; 376.
15. Olea RA. Geostatistics for engineers and earth scientists, Kluwer Academic Publishers. 1999; 303.
16. Isaaks EH, Srivastava RM. An introduction to applied geostatistics, Oxford University Press 1989;561.
17. Orife JM, Avbovbo A. Stratigraphic and unconformity traps in the Niger Delta, in T. Halbouty, ed., the deliberate search for subtle trap: Am. Assoc. Petrol. Geol. Memoir. 1982;32:251-265.
18. Ekweozor CM, Daukoru EM. Petroleum source bed evaluation of Tertiary Niger-Delta. American Association of Petroleum Geologists Bulletin. 1984;70: 48-55.
19. Reijer TJA. Selected chapters on geology, sedimentary geology, sequence stratigraphy: Three case studies: A field guide. SPDC corporate reprographic service, Warri, Nigeria. 1996;194.
20. Tuttle MLW, Charpentier RR, Brownfield ME. The Niger Delta Petroleum System: Niger Delta Province, Nigeria, Cameroon and Equatorial Guinea, Africa. United States Geological Survey, Open-File Report 99-50-H. 1999;65.
21. Burke K, Dessauvagie TF, Whiteman AJ. The Opening of the Gulf of Guinea and the Geological History of the Benue Trough and the Niger Delta; 1971.
22. Whiteman AJ. Nigeria, its petroleum, geology, resources, and potential. 1982; 5(1&2). Edinburgh, Graham and Trotman.
23. Toby D. Well logging and formation evaluation, Elsevier, San Francisco, Calif, USA; 2005.
24. Schlumberger, Log Interpretation, Principle and Application: Schlumberger Wireline and Testing, Houston Texas. 1989;21–89.
25. Udegbunam EO, Ndukwe K. Rock property correlation for hydrocarbon producingsands of the Niger Delta Sand, Oil and Gas Journal; 1988.
26. Asquith N. Basic Well Log Analysis for Geologists. A.A.P.G. Methods in Exploration. Tulsa, Oklahoma. 2004;16: 12–135.
27. Owolabi OO, Longjohn TF, Ajienka JA. An empirical expression for permeability in unconsolidated sands of eastern Niger Delta. Journal of Petroleum Geology. 1994;17(1):111-116.
28. Caers J. Petroleum Geostatistics, Society of Petroleum Engineers: SPE; 2005.

Peer-review history:
The peer review history for this paper can be accessed here:
http://www.sdiarticle4.com/review-history/53873